University of Szeged

Faculty of Medicine, Faculty of Science and Informatics

Department of Medical Physics and Informatics

The evolution of spreading depolarization in response to osmotic or ischemic challenge in rat brain slices

Ph.D. Thesis

Rita Frank

Supervisors: Dr. Ákos Menyhárt

Dr. Eszter Farkas

Doctoral School of Theoretical Medicine

Szeged, 2021

Introduction

Approximately 15 million people suffer a stroke every year, the World Health Organization classifies stroke as the second leading cause of death and the third leading cause of long-term disability worldwide. Stroke cases can either be ischemic or hemorrhagic. The ischemic area can be separated into two major parts: in the ischemic core region, the perfusion is severely decreased, and neurons and glial cells undergo rapid necrosis. The core is surrounded by the penumbra region that is misperfused, and contains electrophysiologically inactive but viable and, most importantly, salvageable cells. These conditions place the penumbra in the center of ischemic neuroprotective therapy. Spreading depolarization (SD) is a slowly propagating wave of near complete neuronal and glial depolarization followed by a temporary suppression of brain electrical activity. After ischemia onset, SD first develops in the core region and spreads through the cerebral grey matter at a rate of 2-6 mm/minute. Massive transmembrane ion movements are typical of SD, such as a rapid increase of $[K^+]_e$ to 30–60 mM, a decrease of $[Na^+]_e$ and $[Cl^-]_e$ to 50–70 mM, and of $[Ca^{2+}]_e$ to 0.2–0.8 mM. In metabolically compromised tissue, the frequency and duration of SDs are in strong correlation with secondary injury development. In experimental models of focal cerebral ischemia, repeated SDs enhance infarct volume, thus SD can be considered as an electrophysiological biomarker of injury progression. Accordingly, pharmacological reduction of SD frequency and/or duration could achieve neuroprotection. Brain edema frequently manifests after the onset of cerebrovascular disorders such as ischemic stroke, and worsens the clinical outcome by increasing intracranial pressure. Cytotoxic edema is defined as intracellular water accumulation without blood brain barrier (BBB) opening, which occurs within minutes after the cessation of cerebral blood flow (Fig.1). During SD, the absence of oxygen and glucose supply induces a disruption of transmembrane ion gradients and leads to the entry of ions and water into the cells. Later, the intensified metabolic crisis transforms cytotoxic edema to ionic edema that lead to altered endothelial ionic gradients, including the transcapillary flux of Na^+ to the brain parenchyma. At this point, astrocytes remain swollen and neuronal death is imminent. Finally, ionic edema transforms to vasogenic edema, in which the complete disruption of cerebrovascular endothelial tight junctions leads to increased BBB permeability to albumin and other plasma proteins. Since, aquaporin-4 (AQP4), the most common water channel in the brain is mainly located on astrocytic endfeet, astrocytes have a critical role in the maintenance of brain water homeostasis. In experimental models of focal cerebral ischemia, the swelling of astrocytes was persistent and correlated with the total duration of spreading depolarization in the ischemic penumbra.

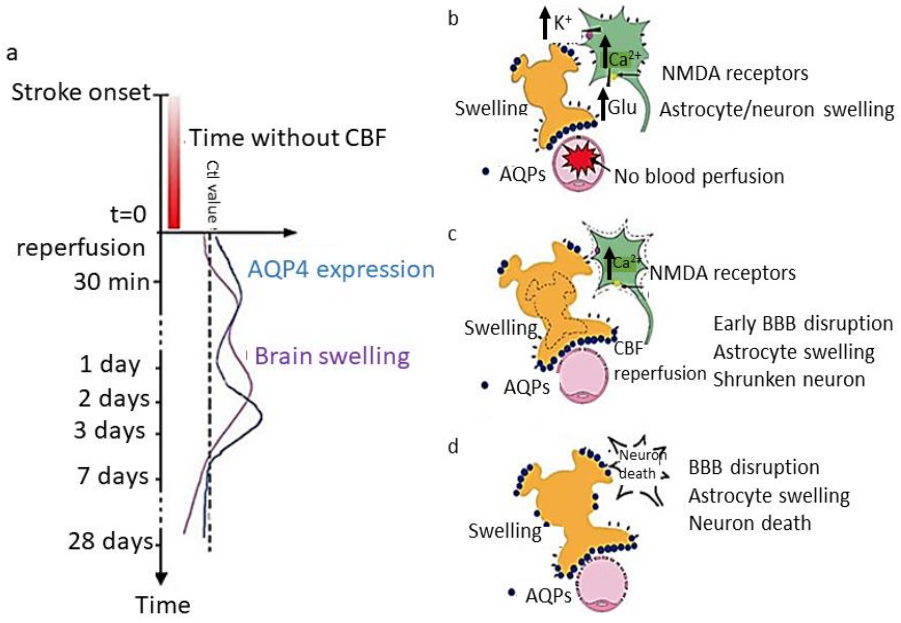

Figure 1. Schematic illustration of edema formation after ischemic stroke (a) Timeline shows edema development after ischemic stroke; the blue trace indicates AQP4 expression, and the purple trace depicts brain swelling after ischemia. **(b)** Cytotoxic edema is characterized as swelling of astrocytes and neuronal dendrites due to the disruption of ion gradients and the entry of ions followed by water influx resulting in cellular swelling mainly through AQP4 channels. **(c)** Ionic edema refers to swollen astrocytes, neuronal death and the leakage of the BBB. **(d)** Vasogenic edema is associated with the disruption of tight junctions between endothelial cells, increased permeability of albumin and other plasma proteins, further swelling of astrocytes and subsequent neuronal cell death (Source: J. Badaut et al. 2011).

Furthermore, astrocytes are essential for neurons and the brain to function optimally, as participants of the tripartite synapse, astrocytes modulate synaptic transmission and neuronal excitability. Astrocytes uptake ions such as potassium and neurotransmitters like glutamate, metabolize them and release their precursors back to neurons. The bumetanide-sensitive $Na^+/K^+/Cl^-$ co-transporter-1 (NKCC1) is particularly implicated in K^+-induced astrocyte swelling. NKCC1 is expressed by astrocytes in all brain regions and its activity is intensified after ischemia. *In vitro* experiments on cultured primary astrocytes demonstrated that NKCC1 contributed to cell swelling in conditions of high extracellular K^+. The control of glutamate clearance is also essential for the modulation of neuronal excitability by astroglia. During synaptic transmission, only 20 % of glutamate binds to postsynaptic receptors, while high proportion of synaptically-released glutamate diffuses out of the synaptic cleft and is cleared from the extracellular space by astrocytic excitatory amino acid transporter-1 (EAAT-1) and EAAT-2. Glutamate uptake is one of the highest energy-consuming mechanisms in the brain, under ischemic conditions when ATP is depleted and the extracellular K^+ is elevated, glutamate

transporters change to reverse mode. In addition, astrocytes may also release glutamate via volume regulated anion channels (VRACs).

In vitro brain slices have been used since the 1950s for the modelling a variety of neurological disorders and to recapitulate the neurophysiological hallmarks of SD accurately. Further, manipulations of the composition of the medium over the preparation allows the controlled simulation of global cerebral ischemia (e.g. oxygen glucose deprivation, OGD) or tissue swelling (e.g. hypo-osmotic medium, HM). Brain slice preparations are an ideal, basic experimental model to test the efficacy of SD inhibiting agents with the goal to achieve neuroprotection. Based on the above, we hypothesized, that; ***(I) SDs significantly decrease the viability of brain cells when tissue homeostasis is disrupted; (II) astrocyte dysfunction due to acute tissue swelling leads to potassium and glutamate accumulation and contribute to ischemic lesion progression.*** In order to prove the presented hypotheses, the following aims were formulated; ***(I) To provide a comparative evaluation of SD evolution in live brain slices, in response to selected SD triggers in dyshomeostatic conditions. (II) To define the role of astrocytes in the evolution of acute tissue swelling, and examine astrocytic glutamate clearance by extracellular glutamate measurements.***

Materials and methods

Young adult, male Sprague-Dawley and Wistar rats (body weight: 250 g; n = 98) were used in these experiments. Coronal brain slices (350 μm) were cut with a vibrating blade microtome. Individual slices were placed in an interface type tissue chamber and continuously perfused with carbogenated aCSF at 32°C. LFP filtered in direct current (DC) mode was acquired via a glass capillary microelectrode which was inserted into the 3rd cortical layer. For IOS imaging, image sequences were captured at 1 Hz with a monochrome CCD camera attached to a stereomicroscope.

Comparative analysis of spreading depolarizations under osmotic or metabolic stress

Methods of SD elicitation

SDs were evoked by pressure injection of 1M KCl (approximately 150 picoliter) or by electric stimulation (50-100 μC). In KCl and ES groups four-to-five successive SDs were initiated in each slice at 10-12 min intervals. Slices were exposed to hypo-osmotic solutions which were prepared by reducing the NaCl concentration of aCSF (HM_{60}-HM_{100}). Slices were incubated in

normal aCSF for 10-15 min before switching to HM superfusion. OGD was induced by superfusion of glucose-free aCSF and the solution was gassed with 95 % N_2 + 5 % CO_2. SDs occurred spontaneously in response to osmotic stress or to OGD.

Histology

The size of the lesion was determined by TTC staining. Images were taken of the cortex with Nikon-DS Fi3 camera attached to a light microscope at 10 x magnification. For proper visualization of cell damage coronal, 10-μm-thick frozen sections were cut from TTC stained slices. The sections were stained with hematoxylin and were examined with light microscopy; photomicrographs at 40 x magnification were taken with a Nikon-DS Fi3 camera.

Observation of simultaneous depolarization on brain slices

Brain slices were exposed to HM as described above. In HM treated slices, after a baseline period, aCSF was replaced with HM in the recording chamber; control slices were incubated in aCSF. The first SD (SD1) was elicited by electric stimulation, and a subsequent, recurrent SD (rSD) was induced by transient anoxia (2.5 min). Hyper-osmotic solution (HRM) contained additional mannitol (100mM) in normal aCSF. To evaluate the impact of HRM slices were incubated in HM, then HM was replaced with HRM. SD1 occurred spontaneously in HM, rSD was elicited by transient anoxia (2.5 min) in HRM.

Pharmacological treatments

Slices were randomly exposed to various pharmacological treatments. For edema reduction, the $Na^+/K^+/Cl^-$ cotransporter blocker Bumetanide (1 mM) and the AQP4 channel inhibitor TGN-020 (100 μM) were co-applied. To inhibit swelling related glutamate efflux via VRAC, slices were exposed to the channel blocker DCPIB (20 μM). NMDA receptors were blocked by MK-801 (100 μM) co-applied with the AMPA/kainate receptor antagonist CNQX (20 μM). TFB-TBOA (10 μM; 100 μM) an EAAT inhibitor was washed on the slices to explore whether glutamate uptake was functional. Fluorocitrate (0.5; 1 mM) a drug that disrupts the citrate cycle in astrocytes was applied to paralyze astrocytes.

Measurement of extra-synaptic glutamate concentration

Extra-synaptic glutamate concentrations were acquired using oxidase enzyme-based microelectrode biosensors. A glutamate biosensor was lowered into the cortex together with an LFP microelectrode and a control sensor covered with bovine serum albumin.

Histology

To examine the morphology and swelling of astrocytes, a modified Golgi-Cox staining was used. Representative images were taken of the superficial cortical layers. For electron

microscopic examination, cross cortical blocks were dissected from representative brain slices. The preparations were contrasted with 5 % uranyl acetate and Reynolds lead citrate solution. The samples were analyzed with a Jeol JEM-1400 Plus transmission electron microscope.

Results

Comparative analysis of spreading depolarizations under osmotic or metabolic stress

First, we compared the electrophysiological features of spontaneous SDs occurring in HM or during OGD to SDs evoked in aCSF. Prolonged SDs and incomplete DC potential recovery were observed during OGD incubation and HM exposure compared to SDs evoked by ES or KCl in aCSF (195.65±117.05 vs. 112.14±88.39 vs. 54.75±26.72 vs. 33.95±26.615 s, HM vs. OGD vs. ES vs. KCl). The incomplete DC potential recovery from SD was also reflected by the reduced slope of repolarization in the HM and OGD groups compared to aCSF (0.30±0.17 vs. 0.12±0.10 vs. 0.50±0.24 vs. 0.45±0.27 mV/s HM vs. OGD vs. ES vs. KCl). The tissue area representing the SD focus was enlarged during HM or OGD incubation compared to ES or KCl-evoked SDs in aCSF (2.64±1.27 vs. 2.23±0.82 vs. 1.93±0.74 vs. 1.37±0.5 % of the total cortical area, HM vs. OGD vs. ES vs. KCl). SDs also invaded a significantly larger cortical area in the HM and in the OGD conditions compared to aCSF (71.98±13.43 vs. 85.32±5.32 vs. 40.4±20.66 vs. 36.72±9.39 % of total cortical area, HM vs. OGD vs. ES vs. KCl). TTC staining was applied to quantify the SD-related tissue injury. We accepted higher numbers of TTC-positive cellular compartments (i.e. particles) to indicate better tissue viability. The SD-related TTC-positive particle loss was obvious after a single SD in HM or OGD (26.45±10.64 and 11.44±6.42 vs. 54.33±21.21 per 1000 μm^2, HM and OGD vs. KCl). Also, the repeated elicitation of SD with ES in aCSF caused a significant reduction in particle number (30.28±9.84 vs. 54.33±21.21 per 1000 μm^2, ES vs. KCl). Corresponding neuronal injury was observed in hematoxylin-eosin-stained sections: condensed, fragmented nuclei and vacuolization indicated pronounced neuronal damage after OGD and HM treatment. This was also seen to a lesser degree after recurrent SDs triggered with ES. In contrast, neurons were preserved and had a large, round nucleus with a prominent nucleolus after repeated, KCl-evoked SDs. Finally, a linear negative correlation was found between the number of TTC-positive particles and the size of the cortical area engaged by SD.

Observation of simultaneous depolarization on brain slices

In our previous *in vivo* experiments we observed that the focus of an SD event became extensive rather than punctual and affected simultaneously an enlarged tissue area during acute ischemic tissue swelling. We termed this phenomenon as simultaneous depolarization (SiD).

To test the hypothesis that acute tissue swelling expands SD focus, we created extreme hypo-osmotic stress to brain slice preparations. SD1 occurred spontaneously during HM incubation or was elicited by electrical stimulation in normal aCSF. Anoxia caused propagating rSD under aCSF incubation, but induced a depolarization involving a larger bulk of tissue simultaneously as opposed to a punctual focus, predominantly in HM (35 of 44 slices, 80%).

IOS recordings revealed that the focus of SD1 was punctual (<1 % of total cortical area) in both aCSF and HM, and was localized to the upper layers of the dorsal-dorsolateral parietal cortex. Anoxia in HM gave rise to SiD in 11 of 16 slices, implicating a sizeable area of the cortex (>50% of the total cortical area), which incorporated much of the tissue previously involved in SD1 propagation. Collectively, these data show that under osmotic stress, the tissue engaged in the propagation of SD1 later turned into a sizeable depolarization focus identified as SiD. The elevated IOS intensity sustained after SD1 and the concomitant failure of complete repolarization from SD1 together predicted SiD occurrence.

To further explore the hypothesis that tissue swelling predisposes the tissue to SiD, we evaluated the degree of tissue swelling caused by the osmotic stress. The increase of the brain slice area was most conspicuous with the second depolarization event, rSD in aCSF and SiD in HM. Under aCSF, the maximum increase of the slice area was greater with rSD than with SD1 (4.75±1.33 vs. 1.09±0.68 pp., rSD vs. SD1), but the swelling was transient and reversible. In HM, slice swelling commenced upon HM exposure, and the slice area gradually increased to reach a considerable expansion already before SD1 (4.59±1.14 and 4.15±1.11 vs. 0.07±0.09 pp., HM_{60} and HM_{100} vs. aCSF). The slice area showed negligible variations afterwards, with no recovery to pre-SD1 level. It is important that slice swelling preceded SD1 and SiD in HM, in contrast with aCSF, in which slice swelling was associated with SD1 and rSD.

Next, since astrocytes rapidly swell in response to hypo-osmotic stress, we hypothesized the pivotal role of astroglial edema in our HM model. Astrocytes appeared clearly swollen in Golgi-Cox-stained slices and electron microscopic preparations after exposure to HM, especially after the passage of SD1. In the electron microscopic images, both the perinuclear cytoplasm and astrocyte processes increased in size.

Consequently, we posited further that swollen astrocytes must substantially contribute to SiD, because astrocyte swelling increases neuronal excitability. The amplitude of evoked potential measured in the cerebral cortex was significantly greater in HM (171.0±11.8 and 184.3±7.4 vs. 93.1±9.3 μV, HM_{60} and HM_{100} vs. aCSF). The latency of SiD occurrence to anoxia onset decreased markedly in HM (46.9±24.3 and 45.9±18.2 vs. 86.9±28.7 s; SiD in HM_{60} and HM_{100} vs. rSD in aCSF). Likewise, the electric threshold of SD elicitation was drastically reduced in HM (50.1±15.7 and 52.5±18.4 vs. 1214.3±470.6 μC, HM_{60} and HM_{100} vs. aCSF). In the latter set of experiments, the implication of astrocyte swelling was confirmed by repeating the SD threshold measurements with the addition of fluorocitrate to the aCSF, which decreased SD threshold similar to HM (51.0±22.9 and 52.5±18.4 μC, fluorocitrate and HM_{100}).

SD has been proposed to recruit viable ischemic penumbra tissue into the infarcted core. Further, persistent cytotoxic edema has been implicated in the SD related dendritic injury. Given this context, we hypothesized that astroglial swelling and the related SiD must have represented the actual tissue infarction in progress. We observed that the maximum depolarized tissue area engaged in SiD was invariably greater than the tissue area traversed by SD1 (76.8±11.4 vs. 60.9±10.7 %, SiD vs. SD1). Macroscopic tissue damage assessed with TTC staining was obvious after SiD compared to SD1 in HM, or aCSF. The number of TTC-positive particles was clearly reduced after SiD compared to SD1 in HM, or aCSF (5.0±1.1 vs. 35.8±3.0 vs. 43.5±1.0 particles per 1000 μm^2, SiD in HM vs. SD1 in HM vs. aCSF). These results suggest that astrocytic edema and the linked SiD seriously jeopardize the survival of neurons and astrocytes. Our data suggest that malignant astrocyte swelling and impaired glutamate clearance drive the expansion of injurious spreading depolarization foci and impose significant damage to the nervous tissue.

Next, we set out to understand the underlying mechanisms of SiD by attempting to prevent it by pharmacological means. Volume regulated or edema-related glutamate release or impaired glutamate clearance emerged as the most likely candidates to promote SiD, because astrocytes have been shown to swell and release glutamate in response to osmotic stress and SD. To test this notion, extracellular glutamate concentration concomitant with slice swelling in HM was measured.

Extracellular glutamate gradually accumulated with slice swelling, to exceed 10 μM concentration by the time SD1 occurred. SD1 was associated with a glutamate peak followed by partially recovery. Then extracellular glutamate concentration remained constantly elevated above 15 μM, coincident with ongoing slice swelling. SiD caused a second glutamate peak with no recovery (>20 μM post-SiD) against a background of marked edema.

Inhibition of astrocyte AQP4 channels and NKCCs by TGN+Bum, or VRACs by DCPIB effectively reduced slice swelling related to HM exposure and SD. Furthermore, TGN+Bum or DCPIB profoundly diminished extracellular glutamate accumulation with SD1 and improved the glutamate recovery after anoxia. Furthermore, both treatments decreased the likelihood of SiD evolution significantly (2 of 16 (13%) vs. 3 of 23 (13%) vs. 28 of 33 (85%) slices; TGN+Bum vs. DCPIB vs. HM_{60}). Instead, the majority of the treated slices gave rise to rSD in response to anoxia. This was reflected in the size of the focal area of depolarization events. While the SD1 focus was punctual and very small (<1 % of the cortical surface) in all groups, the focus of SiD in the HM_{60} group engaged 55.5±7.2 % of the cortex. In contrast, the rSD focus in the TGN+Bum and DCPIB groups was much more confined. Taken together, the inhibition of astrocyte swelling by TGN-020 + Bum or DCPIB evidently blocked SiD evolution.

Next, we asked whether astrocyte dysfunction is sufficient to produce the SiD phenotype in normal aCSF. Fluorocitrate treatment to arrest astrocyte metabolism replicated slice pathology in HM; (i) the SD elicitation threshold decreased; (ii) SD1 emerged spontaneously (4 of 5 slices), and (iii) SiD evolved upon subsequent anoxia (3 of 5 slices). In line with these data, inhibition of astrocyte EAAT2 caused profound extracellular glutamate accumulation to 29.5±9.9 μM, which was followed by a SiD (3 of 4 slices). Extracellular glutamate accumulation with SiD peaked at 65.3±18.1 μM, followed by further extracellular glutamate accumulation without any recovery. These data further substantiated that extracellular glutamate accumulation must have mediated SiD in HM.

To determine the source of surplus glutamate accumulated in the extracellular space during tissue swelling AMPA, NMDA and kainate receptors were blocked. The antagonism of ionotropic glutamate receptors was partially effective against SiD, but was ineffective against slice swelling in HM. Furthermore, glutamate receptor antagonists were the least effective against extracellular glutamate accumulation. These observations confirmed the pivotal role of astrocytes in tissue swelling and suggest that surplus glutamate of astrocyte origin, in addition to neuronal release, must be implicated in the evolution of SiD.

Taken the results above, we hypothesized that the complete reversal of cellular edema by hyperosmotic treatment could restore extracellular glutamate levels to the physiological range and prevent SiD. HRM completely reversed slice swelling, restored physiological extracellular glutamate concentration, and promoted the recovery of the IOS signal. Further, HRM exposure completely prevented the occurrence of any depolarization and extracellular glutamate accumulation upon anoxia. The electrical threshold of SD elicitation was also markedly

increased under HRM (2422.5±341.7 vs. 54.0±2.1 vs. 1220.0±6.2 μC, HRM vs. HM_{100} vs. aCSF). The coincidence between slice swelling and extracellular glutamate concentration was further supported by their strong positive linear correlation (r=0.819**). We concluded that extracellular glutamate content was tightly coupled to tissue edema, and that anti-edema treatment effectively counteracted extracellular glutamate accumulation and SiD.

Discussion

Comparative analysis of spreading depolarizations under osmotic or metabolic stress

Here we set out to provide a comparative analysis of SD evolution on live brain slices, in response to selected SD triggers and in various media, under otherwise standardized experimental conditions. In this experimental project we aimed to explore the electrophysiological together with the intrinsic optical signal features of SDs under global oxygen-glucose deprivation or osmotic stress with respect to the physiological condition. The histological consequences of SD under these states were also evaluated.

The application of OGD to study SD was justified by its widespread use to mimic severe global ischemia (e.g. cardiac arrest) or conditions prevalent in the ischemic core in focal cerebral ischemia. To study the impact of osmotic stress on SD, we incubated the brain slices in HM, following a previously established approach to model cerebral edema progression. Finally, as control for both OGD and HM, we elicited SD in aCSF with highly focused KCl pressure injection, expected to be near the minimum conditions of SD elicitation, and the least invasive. This condition is thought to be relevant to model SD as it occurs in migraine with aura. In other aCSF-incubated slices, electrical stimulation was applied for SD elicitation, due to its frequent application in some labs with the purpose to determine the threshold of SD elicitation.

Both OGD and HM gave rise to a spontaneous, long-lasting SD, at a short latency as previously shown. These spontaneous events propagated over the entire cortical area in the preparation. The brain slice was irresponsive to further stimulation after SD in OGD, and displayed acute, extensive histological damage in the path of SD. In contrast, the tissue repolarized from the SD in HM – albeit with a long delay. The first SD in HM caused cellular injury in the cortex engaged in SD, but the damage was less severe than that seen after SD in OGD. SD evoked by OGD sustained for 15-20 min here was associated with extensive injury in all layers of the cortex as evidenced by TTC staining, and in line with previous reports. In the control conditions here (KCl or ES), a train of 4-5 short-lasting SDs could be elicited at an interval of 10-12 min,

which demonstrates the sustained viability of the tissue after the passage of SD under physiological conditions. Of the two control conditions here, focal low volume KCl application with pressure injection caused no detectable histological degeneration in the brain slice. However, ES-triggered SDs were accompanied with obvious damage to the tissue. Although not documented systematically, most SD researchers agree that electric stimulation with a charge sufficient to trigger SD leaves focal necrotic tissue damage behind at the electrode contact point.

Collectively, our results here present three stages of the SD continuum: (i) apparently harmless SD in intact tissue followed by sufficient repolarization and recovery, (ii) injurious SD with poor repolarization and recovery emerging under osmotic stress, and (iii) terminal and detrimental SD with no repolarization in oxygen and glucose deprived tissue. The distinct features of the negative DC shift and IOS signature of SD may disclose some mechanistic elements of SD evolution typical for the homeostatic conditions. For example, the slower rate of repolarization in HM and OGD as seen here is thought to correspond to the dysfunctional re-uptake of K^+ or glutamate. The shortage of ATP in OGD causes the failure of the neuronal and astrocytic Na^+/K^+ ATP-ase, which hampers the uptake of K^+ accumulated with the SD wave front in the extracellular space. HM exposure has been shown to induce prominent astrocyte swelling and to disrupt the astrocyte buffer capacity, reflected by a progressive accumulation of glutamate, for example. Astrocytic K^+ and glutamate re-uptake has been implicated in the repolarization after SD. Taken together, we propose that the plausible cause of slower repolarization and prolonged SD duration in HM was the injured glial K^+ clearance and glutamate transport. The failure of the Na^+/K^+ ATP-ase and the exhaustion of the astroglial buffer capacity are also suspected to contribute to the remarkably greater area engaged in SD propagation in HM and OGD compared to aCSF.

Observation of simultaneous depolarization in brain slices

Next, we performed extensive pharmacological manipulations and electrophysiological recordings together with extracellular glutamate measurements and histological analysis to understand the mechanistic background of SD in acute tissue swelling.

Here we present novel observations in brain slices that the simultaneously depolarized tissue volume denoting the focus of an SD event (i.e. simultaneous depolarization, SiD) may become extensive (>2 mm^2) rather than punctual (<1 mm^2) during acute ischemic tissue swelling. We demonstrate that malignant astrocyte swelling promotes SiD evolution and neuron death in our edema model. We further show that SiD encompasses tissue that has previously participated in

the propagation of an SD, causing the subsequent aggravation of histological damage. However, the mitigation of astrocyte swelling by pharmacological treatment or by hyper-osmotic therapy prevented SiD.

Cerebral edema produced experimentally is a sufficient condition for SD to occur spontaneously, which predisposes the tissue covered by the propagating SD for an upcoming SiD. The tissue volume engaged in the SiD then serves as an extensive focus of an SD event taking off from its perimeter. In particular, SiD is predicted by the swelling of astrocytes in edematous tissue. Astrocyte swelling under hypo-osmotic stress is implicated in the excessive extracellular accumulation of glutamate, coincident with SiD occurrence. Further, SiD is followed by the oncotic cell death of neurons and astrocytes, suggestive of injury maturation associated with SiD.

These are the first experiments to characterize SiD comprehensively. SiD-like events were recorded previously in brain slice preparations incubated in hypo-osmotic medium and challenged with hypoxia, but without detailed analysis of the phenomenon or realizing its significance. It is of high importance that an SiD-like event has been recently captured in the severely injured human brain. In the ischemic penumbra of a malignant hemispheric stroke, terminal depolarization in the wake of circulatory arrest was seen to arrive with an unusual short delay from electrode to electrode on the subdural strip, when the strip was positioned at an already compromised area of the cortex. This observation suggests that SiD is clinically relevant and gives ample momentum to study the pathophysiological relevance of SiD in more detail.

Brain slices were exposed to severe osmotic stress achieved by the lowering of $[Na^+]$ of the incubation medium to 100 or 60 mM. SiD in our study occurred invariably superimposed on tissue edema, a condition to affect astrocytes first. The attention to astrocytes was also substantiated by our finding that fluorocitrate treatment caused astrocyte swelling and reproduced SiD evolution. Astrocytes are more permeable to water than neurons because astrocytes are endowed with AQP4 water channels at their processes, which conduct osmotically driven water. Further, astrocytes have been found to swell in response to ischemia or SD, which is thought to represent water movement via AQP4 along inward K^+ currents. Alternatively, neurons and astrocytes are both affected by the SD-related cytotoxic swelling due to excess chloride entry through NKCC. We found that HM-exposed astrocytes were markedly swollen in histological preparations, and that the blockade of AQP4 channels and NKCCs prevented tissue edema and SiD occurrence under hypo-osmotic stress. These data collectively demonstrate that astrocyte swelling must be central to SiD evolution. Astrocytic

swelling has been implicated in volume regulated glutamate release through glutamate-permeable VRACs. At the same time, the significant glutamate uptake through astrocytic Na^+- and ATP-dependent EAAT2 is impaired under metabolic stress, which sustains high extracellular glutamate concentration. The inhibition of VRACs in our experiments prevented the extracellular accumulation of glutamate, reduced the focal area of depolarization and the likelihood of SiD occurrence. Conversely, EAAT2 blockade alone reproduced the SiD phenotype as seen under HM incubation. The antagonism of AMPA and NMDA receptors was partially effective against SiD, and resulted in multifocal SD evolution. These results suggest that surplus extracellular glutamate of astrocyte origin, in addition to neuronal release, must be implicated in the evolution of SiD. Previous observations suggest that even with only a very low residual blood flow, SD must last longer than 10 min before cell death occurs. Our histological results suggest that this time span is significantly shortened when astrocytic function is already disturbed before the onset of neuronal depolarization. Thus, although SD is a primarily neuronal phenomenon, our findings substantiate the outstanding importance of astrocytes as protective guarantors against the devastating effects of SD.

The clinical management of cerebral edema in acute brain injury currently aims at the reduction of intracranial pressure and the maintenance of cerebral perfusion pressure by sedation, hyperventilation, osmotherapy, hypothermia, and in the most severe cases decompressive craniectomy. However, for example, in severe subarachnoid hemorrhage intravenous high sodium fluids are administered increasingly more frequently because hypo-osmolarity is suggested to increase the risk and severity of delayed ischemic injury.

Acknowledgements

Firstly, my acknowledgment is dedicated to my supervisors Dr. Ákos Menyhárt and Dr. Eszter Farkas. I am thankful to Ákos for his constructive ideas, directions and his never-ending help during my doctoral training. I am very thankful to Eszter who allowed me to join her research group and with her guidance and advices helped me to accomplish my experimental projects and my thesis.

I would like to recognize the help and support of my current and ex-colleagues and also friends in the lab: Dr. Írisz Szabó, Dr. Dániel Péter Varga, Dr. Viktória Éva Varga, Dr. Orsolya M. Tóth, Anna Törteli, Dr. Réka Tóth, Dr. Szilvia V. Kecskés, Dr. Armand Rafael Bálint, Orsolya Ivánkovitsné Kiss, Dr. Péter Makra.

I would like to thank Prof. Dr. Ferenc Bari for enabling and supporting my work at the Department of Medical Physics and Medical Informatics. I would also like to thank to Prof. Dr.

Ferenc Peták for supporting my work in the Department of Medical Physics and Medical Informatics.
I would like to say grateful thanks to Prof. Dr. József Toldi and Dr. Kitti Kocsis for introducing me to the world of science and laboratory work.
And last, but not least, words cannot describe how grateful I am to my parents and my brother for their unbreakable help and support. I thank from the bottom of my heart my husband Tomi for never letting me down and for being there always.

Articles to serve as the basis of the thesis:

1. **Rita Frank**, Ferenc Bari, Ákos Menyhárt, Eszter Farkas *Comparative analysis of spreading depolarizations in brain slices exposed to osmotic or metabolic stress.* BMC Neuroscience 2021 May 3;22(1):33. doi: 10.1186/s12868-021-00637-0. **IF: 3.288**

2. Ákos Menyhárt [a], **Rita Frank [a]**, Attila E. Farkas, Zoltán Süle, Viktória É. Varga, Ádám Nyúl-Tóth, Anne Meiller, Orsolya Iványkovits-Kiss, Coline L. Lemale, Írisz Szabó, Réka Tóth, Dániel Zölei-Szénási, Johannes Woitzik, Stephane Marinesco, István A. Krizbai, Ferenc Bari, Jens P. Dreier, Eszter Farkas *Malignant astrocyte swelling and impaired glutamate clearance drive the expansion of injurious spreading depolarization foci* Journal of Cerebral Blood Flow and Metabolism August 24, 2021., DOI: 10.1177/0271678X211040056 **IF: 6.200**